Stretching of Solution Processed Carbon Nanotube and Graphene Nanocomposite Films on Rubber Substrates

Sampo Tuukkanen[a,*], Maija Hoikkanen[b], Minna Poikelispää[b], Mari Honkanen[b], Tiina Vuorinen[a], Markus Kakkonen[b], Jyrki Vuorinen[b], Donald Lupo[a]

[a] *Tampere University of Technology, Department of Electronics and Communications Engineering, Korkeakoulunkatu 3, FI-33720, Tampere, Finland*
[b] *Tampere University of Technology, Department of Materials Science, Korkeakoulunkatu 6, FI-33720, Tampere, Finland*

Abstract

The fabrication and characterization of stretchable carbon nanotube and graphene nanocomposite electrodes on different rubber substrates is reported. Electrodes are fabricated at low temperatures using solution processable carbon nanomaterials. Rubber substrates are stretched while performing simultaneous electrical measurements for the electrodes. During 20 % elongation of rubber substrates a 2–120-fold increase in the electrode resistance was observed, depending on the sample. The relative increase in the resistance with stretching was smaller in the case of graphene electrodes, whereas the resistance change during the elastomer relaxation was smaller in the case of carbon nanotube electrodes. Our results suggest that solution processed carbon nanomaterials on rubber substrates have potential for stretchable wiring and sensor applications.

Keywords: Carbon nanotubes A, Flexible composites A, Polymer-matrix composites (PMCs) A, Electrical properties B, Stress/strain curves B

1. Introduction

Carbon-based nanomaterials, especially carbon nanotubes (CNT) [1] and graphene [2], have gathered exceptional interest during the last decade due to their properties such as high electrical and thermal conductivity, high tensile strength, high surface area, chemical sensitivity, flexibility, transparency, light weight and environmental friendliness. Graphene and CNTs have already shown their potential in the fields of electronics [2–4], optoelectronics [1, 3, 5] and materials technology [6, 7] as well as in energy technology and biotechnology [8]. For example, the electrical conductivity and high surface area make graphene and CNTs interesting for supercapacitors [9–12] which are potential future energy storage devices. The potential transparency of these materials enables their use in solar cells [13–15] and displays [16] or as transparent electrodes in transistors [17] or sensors [18, 19], whereas chemical sensitivity makes them efficient sensing materials [20]. The elasticity, mechanical stability and high conductivity make graphene and CNT networks especially interesting for flexible [4] and stretchable electronics [21, 22] as well as composite technology [6, 22, 23].

Utilization of printing technologies for the fabrication of electronics has raised interest in both academic and industrial communities. Printing technologies offer a promising route for low-cost and high-throughput manufacturing of flexible, lightweight and even transparent electronic devices [24], such as flexible displays, radio frequency identification (RFID) antennas, batteries, supercapacitors and solar cells [25, 26]. The use of printing technologies in combination with disposable, non-toxic organic and molecular materials can lead us towards green electronics [27]. These types of devices have numerous potential applications in future electronics, such as logistics, energy harvesting and ambient intelligence.

Despite their intrinsic tendency to aggregate, graphene and CNTs can be made solution processable by using chemical modification [28, 29] or solubilizing additives, such as surfactants, cellulose derivatives [9, 30, 31] or conducting polymers [32]. This has enabled the solution-based processing of carbon nanomaterials [4, 28, 33] and the fabrication of devices using printing techniques [17, 18, 34, 35].

Composites of rubber and CNTs have been widely studied in order to improve the mechanical durability [36–40] as well as electrical [37, 40, 41] and thermal conductivity [38, 42] of the rubber. A composite of rubber and graphene has also been recently demonstrated [43]. If a carbon nanomaterial is used as a sensing material or an electrode, instead of a composite material, only a thin film on the rubber substrate is required. For this type of application, thin graphene and CNT films can be produced easily with printing techniques, which allows a high-throughput fabrication process and minimal consumption of the electrode material. The use of solution processed CNT films for flexible [4] and stretchable electronics [22] has been extensively studied, but there are only a few demonstrations of solution processed graphene electrodes on flexible [44] or stretchable substrates [45]. For the deposition of CNTs on elastomer substrates, a so-called buckling process has been developed [21, 46]. In these studies, poly(ethylene terephthalate)

*Corresponding author. Tel.: +358 405415276.
Email address: sampo.tuukkanen@tut.fi (Sampo Tuukkanen)

(PET) has been generally used as a flexible substrate, whereas poly(dimethylsiloxane) (PDMS) silicone has been used as a stretchable substrate [47]. However, an extensive study of solution-processed graphene or CNT films on rubber substrates has not been reported.

In this paper, we demonstrate the fabrication of solution-processed graphene and CNT electrodes on different rubber-based substrates. The electrical conductivity of nanocarbon films has been measured with simultaneous rubber elongation. Films made from graphene and CNT inks have been compared in the cases of four different rubber substrates. The microstructure of the printed films was studied by microscopic methods.

2. Experimental

Two different types of solution processable carbon nanomaterials, i.e. graphene and CNT, were deposited as stretchable electrodes on four different types of rubber substrates. The substrates were stretched while performing simultaneous electrical measurements for the nanocarbon electrodes. The samples were characterized using electrical, microscopic and mechanical analysis.

2.1. Rubber substrates

Four elastomer-based rubber materials containing different fillers were used as substrates; (*1*) NR/BR 15 phr clay, (*2*) NR/BR 25 phr carbon black, (*3*) NBR unfilled and (*4*) CSM. The base elastomers were selected to represent a mixture of different chemical structure and mechanical properties, as no previous knowledge on the substrate selection was available. Blends of natural rubber (NR) and butadiene rubber (BR) are commonly used in technical applications such as tyres; the rubbers *1* and *2*, having different filler systems, represent stiff and more flexible (soft) variants, respectively. In addition, due to the electrically conductive filler, the electrical conductivity of rubber *2* is higher than the electrical conductivity of rubber *1*. Rubber *3* was nitrile-butadiene rubber (NBR), which is tough and has a good chemical resistance. Rubber *4* was chlorosulphonated polyethylene (CSM) which has high temperature, oil and outdoor resistance but average mechanical properties. Rubbers *1–3* were fabricated in-house while rubber *4* was a commercial compound. Elastomers *1–3* and their ingredients (filler, ZnO and stearic acid) were mixed in internal mixer Brabender N 350 E and the curatives were added on two-roll mill. All samples were vulcanized to 2–3 mm thick sheets by compressing moulding with their respective curing time (t_{90} + 2 min). Tensile properties were determined according to ISO 37 with dumbbell specimen type 1. Tests were performed with Messphysik Midi 10-20 universal tester and contact extensometer. The Shore A hardness was recorded according to ASTM D 2240–00 with AFFRI Hardness tester. Surface energy measurements for the rubber substrates were performed using a CAM 200 goniometer (KSV Instruments). Mechanical properties and surface energies of the rubber substrates are presented in Table 1.

The rubber substrates were cut to suitable size pieces for stretching experiments (discussed in Section 2.6). The rubber samples had a length of 60–80 mm, thickness of 2.0–2.5 mm and width of 19–28 mm. The sample dimensions are needed when calculating the resulting stress applied on each sample from the applied stretching force.

Prior to the electrode deposition, the rubber samples were stretched up to 120 % length (20% elongation) with a universal testing machine (Instron 5967) and then let return to their initial length. This was done to remove tensile stress-softening, i.e. Mullins effect [48, 49], which makes the actual rubber stretching experiments more repeatable.

2.2. Inks

One graphene ink and one CNT ink were used for deposition of the electrodes on the rubber substrates. The graphene ink (denoted *X* in the following sections) was a commercially available ink formulated especially for screen printing (P3014 Graphene Screen Printing Ink from Innophene Co., Thailand). The CNT ink (denoted *Y* in the following sections) is a nanocomposite material which was prepared by mixing CNTs and cellulose derivatives with ultrasonication (obtained from Morphona Ltd., Finland). The solid content of the ink was 1.5 wt-% and its preparation procedure was similar to one described previously [31].

2.3. Fabrication of electrodes

Both inks were deposited on the rubber substrates using blade-coating method. Patterning of 1 cm by 5 cm stripes was done with a mechanical mask. For the graphene ink, a mask was made of 7 layers of Scotch tape (total thickness about 380 μm). For the CNT ink, a mask was made from 125 μm thick PET film which was attached to the substrate using adhesive tape. After deposition the films were dried in a convection oven. The graphene films were dried for 7 min and the CNT films for 5 min at 130 °C. The final thicknesses of the graphene and CNT films were 3–5 μm and approximately 1 μm, respectively (see Section 3.3). The electrode thicknesses were selected so that obtained sheet resistances were approximately the same for both materials, which makes the analysis of the results more consistent (see Table 2).

2.4. Sheet resistance measurements

The sheet resistances of fabricated nanocarbon films were measured using a four-point probe setup and a multimeter (Keithley 2425 100 W SourceMeter) [31]. The four probes were placed in line with an equal spacing of 3 mm between them. The value for the sheet resistance is given by

$$R_S = G\frac{\pi}{\ln 2}\frac{V}{I},$$

where G is the additional geometric correction factor, which depends on sample dimensions and the probe spacing [50]. Measured sheet resistances for the nanocarbon electrodes are presented in Table 2. Sheet resistance measurements were also performed for the bare rubber substrates to ensure that they do not contribute to the electrical conduction. All rubber substrates showed highly insulating behaviour giving the sheet resistance $R_S > 1$ GΩ/□.

2.5. Adhesion test method

The adhesion of deposited nanocarbon films on the rubber substrates was studied before and after the stretching experiments using the tape test method. Adhesion classification is done according to ASTM standard D 3359-97 (Standard Test Methods for Measuring Adhesion by Tape Test) by applying and removing pressure sensitive tape over cuts made in the ink [51]. In Test Method B, classification 5B refers to the case where adhesion is very good and no material is detached from the film. Classification 0B refers to the case where over 65 % of the material has detached from the film. Results of the adhesion tests are presented in Table 2.

2.6. Stretching experiment procedure

Stretching of the rubber samples with nanocarbon electrodes was done using the universal testing machine Instron 5967 that could be programmed for all the cross head movements needed in the tests. A schematic view of used experimental setup is shown in Figure 1.

In the rubber stretching experiments, the samples were stretched in a stepwise manner. Rubbers were stretched up to 120 % length (20 % elongation) at speed of 5 mm/min with 15 seconds breaks at every 1 % (of absolute value) elongation intervals. In other words, after each stretching step (20 stretching steps in total) the rubber sample had time to relax for 15 seconds.

Electrical measurements were performed on the nanocarbon electrodes while the samples were simultaneously stretched. The two-probe resistance of the film at a 1 cm distance was measured using a multimeter (Keithley 2425) and the resistance values R were collected in the beginning and in the end of each stretching step. Pieces of copper film were used to make electrical contact to the nanocarbon electrodes on the samples. Clips were used to keep to the copper pieces in contact with the samples during the elongation experiment. The copper was used as a contact metal because it has been reported to give reasonably low contact resistance with CNTs [52].

Simultaneously collected stress and resistance values R are plotted in Figure 2. The results of stretching experiments are summarized in Table 3. The resistance R_{before} was measured before the stretching experiments was started and R_{after} after the experiment when the sample was let to return to its original length. The value $R_{\text{final}}/R_{\text{initial}}$ refers to the relative change of the resistance R during the stretching experiment.

The gauge factor (GF) for a strain sensor is defined by

$$GF = \frac{\Delta R/R_{\text{initial}}}{\Delta L/L} = \frac{R_{\text{final}}/R_{\text{initial}} - 1}{0.2}$$

where $\Delta R = R_{\text{final}}$-$R_{\text{initial}}$ is a change of the resistance from its initial resistance value R_{initial}, ΔL is an absolute change in length and L is the original length of the sample.

2.7. Microscopic analysis

After the stretching experiments, photographs and optical microscope (Olympus BX 51) images were taken from all samples both straight and bent. While imaging the bent samples were fixed in place under the objective using an adhesive tape. Bending was done to simulate the stretching of the substrate from the electrode's point of view.

To analyse the microstructure of the graphene and CNT electrodes, the samples were imaged using a scanning electron microscope (SEM, Zeiss ULTRAplus) and a transmission electron microscope (TEM, Jeol JEM-2010). For the SEM analysis, the samples were cut at the middle of the electrodes. While SEM imaging, the samples were tilted 40° to study the cross section of the electrodes. For TEM imaging, pieces of graphene and CNT ink films were detached from the rubber substrates and placed between folding TEM grid.

3. Results and discussion

The graphene and CNT electrodes were blade-coated on four different types of rubber substrates. After the deposition of nanocarbon films, the adhesion tests and sheet resistance measurements were performed for the films. The conductivity measurements were performed for the electrode areas that were used for the subsequent stretching experiments, while the adhesion tests were performed for the regions that were not used for the electrical measurements. The rubbers were then stretched while simultaneously measuring the electrical conductivity of the nanocarbon films in order to analyse how the stretching affects the conductivity of the films. After the stretching experiments, the samples were analysed using optical and electron microscopy.

3.1. Analysis of fabricated electrodes

The results of sheet resistance measurements performed after the electrode deposition and the results of adhesion tests performed before and after the stretching experiments are shown in Table 2. The sheet resistances measured after electrode deposition were quite similar for all samples, as was expected due to the suitable selection of film thicknesses. This indicates that blade-coating is a reproducible way to fabricate homogeneous graphene and CNT electrodes on rubber substrates.

By comparing the values in Table 2, one can conclude that a better adhesion and good quality films were obtained in the cases of higher surface energy rubber substrates (rubbers *3* and *4*). It also seems that good adhesion and higher surface energy results in lower sheet resistance values (higher conductivity). The adhesion tests before and after stretching showed that adhesion either decreased or remained the same during stretching, which suggests that the stretching caused detachment of the electrode material from the rubber with certain material combinations.

3.2. Analysis of stretching experiments

The results of the stepwise stretching with simultaneous resistance measurements are shown in Figure 2. Open circles in the plots show the collected resistance values in the beginning and in the end of each stretching step. The zig-zag shape in the measured stress curves can be explained by relaxation of the rubber during the paused between each stretching steps.

Samples *X-1* and *X-4* could not be measured because the resistance in those was over the measurement range of the multimeter range ($R > 20$ MΩ) already in the beginning of the stretching experiment. After the experiments, electrodes on these samples contained visual cracks which were most likely formed in the beginning of the stretching experiment or sample handling.

The stress curves for rubber *2* (samples *X-2* and *Y-2*) look the same with each other. The same can be seen in the case of rubber *3* (samples *X-3* and *Y-3*). Therefore, the deposited thin film electrodes do not change the stress-strain behaviour of rubber substrates.

From stress vs. time curves one can notice that a drop in the stress during the stretching breaks was smaller in the case of rubbers *1* and *3* (samples *X-3*, *Y-1* and *Y-3*) which have a low modulus (See stress at 100 % elongation in Table 1). This can be interpreted as a relaxation of the rubber during the pause. Relaxation results are summarized in Table 3.

The resistance values measured before (R_{before}) and after (R_{after}) the stretching experiment (when the sample was not attached to the stretching tool) are presented in Table 3. When comparing these values, one can notice that in the samples *X-2* and *Y-2* there was a 4-fold and 2-fold increase in the resistance, respectively. In the rest of the samples, the resistance returned almost to the initial level measured before the stretching. This suggests that rubber *2* is not a suitable substrate for these printable materials as least when considering stretchable and reversible electrode applications. However, substrates *1*, *3* and *4* gave promising results.

It can be observed from Figure 2 that resistance R rises quite linearly during the stretching in samples *X-2*, *X-3* and *Y-2*, whereas in samples *Y-3* and *Y-4* the resistance rise is exponential. In sample *Y-1* there is a jump in the resistance in the beginning of the measurement, after which it rises linearly. In samples *X-2*, *X-3* and *Y-1* there are more differences between the resistances measured in the beginning and in the end of the pause (between stretching steps). This could be partially explained by the relaxation of the rubber at least for samples *X-3* and *Y-1*, where a stronger relaxation was observed during the pause.

The relative resistance change $R_{\text{final}}/R_{\text{initial}}$ presented in Table 3 was calculated from the resistance monitoring results by dividing the resistance at the end of stretching by the resistance value at the beginning of the stretching. The relative resistance change in the case of graphene electrodes was from 1.5–4-fold, whereas in the case of CNT electrodes it was from 8–120-fold. One reason for this can be that the graphene film was 5 μm thick and CNT film only 1 μm thick, which allows more conduction routes for graphene during electrode elongation. Also, the ink compositions were different: the CNT ink contained insulating cellulose derivatives whereas the graphene ink contained a certain amount of conducting polymer, which improves the conductivity of the film. The gauge factors (GF) calculated from the experimental results are shown in Table 3.

An ideal elastic conductor with the volume $V = A \cdot l$ has the resistance $R = \rho \cdot l/A$, where A is the cross-sectional area, l is the length of the conductor and ρ is the resistivity. If we assume, as a good approximation, that the volume and resistivity of the elastic conductor stays the same during the elongation, the resistance would be $R = \rho \cdot l^2/V$. This means that the resistance should increase in the power of two with length. At the end of a 20 % elongation experiment, the resistance should be 1.44 times larger than in the beginning, which is about the same as was observed in the case of graphene electrode sample *X-3*. In other samples the increase of the resistance was larger. One can also observe that most of the resistance curves in Figure 2 do not increase in the power of two with length (the same as time axis in this case) but more or less linearly, at least in the beginning of the elongation. This means that the nanocarbon network does not behave like a elastic conductor, but more like a reorganising nanowire network where resistance increases as the number of percolation paths decreases.

3.3. Microscopic analysis of the samples

After the stretching measurements, visual and microscopic analysis was performed for all samples to obtain further information about the behaviour of the electrodes on rubber substrates. Samples were imaged as straight and while bent to simulate the effect of stretching. The photographs and optical microscope images are shown in Figure 3. The microstructure of the electrode materials can be analysed from the SEM and TEM images shown in Figures 4 and 5, respectively.

SEM images of the cross-sections of the graphene and CNT electrodes (samples *X-2* and *Y-1*) on the rubber substrates are presented in Figure 4. The thicknesses of the electrodes were measured from SEM images: the graphene electrodes were 3–5 μm thick and the CNT electrodes approximately 1 μm thick. All different substrates containing the same electrode material looked similar in SEM analysis.

TEM images of the graphene and CNT electrodes (samples *X-3* and *Y-1*) are presented in Figure 5. In Figure 5(a) one can see graphene flakes dispersed in the polymer matrix. This was confirmed from the diffraction pattern (data not shown here) which indicated that both amorphous and crystalline components were present in the material. From Figure 5(b) one can see that CNTs are very homogeneously distributed in the cellulose matrix, which indicates the high stability of the CNT nanocomposite ink. In TEM analysis, all the samples containing the same electrode material showed the same microstructure.

In general, one can conclude that the behaviour of the graphene ink was highly dependent on the substrate material, whereas the CNT ink film behaved quite similarly on all substrates. Most of the samples were not harmed during the stretching experiments. However, some of the electrodes were cracked while stretching, which can also be observed from the photographs taken from the bent samples in Figure 3. The increase in the electrode resistance shown in Table 3 suggests a deterioration of the electrodes during the stretching.

High quality films with low resistances were obtained in the cases of high surface energy rubbers *3* and *4*. Samples *X-3*, *Y-3* and *Y-4* had good quality films, such as shown in Figures 3(a) and (b), which showed low resistivity also after stretching experiments. However, sample *X-4* showed high resistance in the

beginning of the stretching experiment, which may be due to deep cracks observed in the microscope image of the bent sample in Figures 3(e).

The electrodes deposited on rubbers *1* and *2* were not as good quality as on rubbers *3* and *4*, which is most likely due to higher roughness of the substrates as can be observed visually from Figures 3(c) and (d). In the graphene ink samples *X-1* and *X-2*, the quality of the electrodes was quite poor. Even though sample *X-1* appeared fine after electrode deposition, it could not be used in the stretching experiment since some cracks which can be seen in Figure 3(c) appeared in the beginning of the experiment. The electrodes on the sample *X-2* contained some bubbles already after electrode fabrication, but it was still usable for the stretching measurements. However, the bubbles caused higher resistances both before and after stretching as can be seen from Table 3. Also cracks appear in the electrodes as can be observed in Figures 3(d) and 4(a).

The CNT ink samples showed good performance in the cases of all four rubbers and their resistance before and after the stretching was about the same as can be seen from Table 3. This was also supported by the microscope study. Samples *Y-3* and *Y-4* showed high quality films as shown in Figure 3(b). Deep cracks through the whole film were not observed either in samples *Y-1* and *Y-2*, as can be seen from Figure 3(f).

The microscopic studies suggest that the nanocarbon electrode material behaviour on the rubber substrate depends strongly on the compatibility of the substrate and electrode materials. Their material interactions, such as the adhesion between materials as well as the cohesion of the nanocarbon electrodes, determined the behaviour while stretching the rubber. Observed resistances measured before and after the stretching experiment also support these results.

Our results suggest that solution processed graphene and CNT films on rubber can be used as stretchable electrodes or as sensors when suitable material combination is selected. This opens up new application areas for rubbers combined with nanostructural carbon materials. For example, stretchable conducting coverage for elastomer products such as automotive tyres as well as various sensor applications can be considered.

4. Conclusions

Both graphene and CNT worked well as electrodes on most of the rubber substrates. The relative resistance change during the stretching is larger and rubber relaxation after the stretching affects less to the resistance in the case of CNT electrodes. This makes the CNT films more suitable for sensor applications where varying stress is applied to the element. On the other hand, the smaller relative resistance change during the stretching of the graphene electrodes would make them applicable to be used as stretchable electrodes.

5. Acknowledgements

S. Tuukkanen acknowledge the funding from the Academy of Finland (Dec. No. 138146).

References

[1] Robertson J. Growth of nanotubes for electronics. Materials Today 2007;10:36–43.
[2] Geim AK, Novoselov KS. The rise of graphene. Nature Materials 2007;6:183–91.
[3] Avouris P, Chen Z, Perebeinos V. Carbon-based electronics. Nature Nanotechnology 2007;2:605–15.
[4] Park S, Vosguerichian M, Bao Z. A review of fabrication and applications of carbon nanotube film-based flexible electronics. Nanoscale 2013;5(5):1727–52.
[5] Bonaccorso F, Sun Z, Hasan T, Ferrari AC. Graphene photonics and optoelectronics. Nature Photonics 2010;4:611–22.
[6] Paul DR, Robeson LM. Polymer nanotechnology: Nanocomposites. Polymer 2008;49(15):3187–204.
[7] Lee C, Wei X, Kysar JW, Hone J. Measurement of the elastic properties and intrinsic strength of monolayer graphene. Science 2008;321(5887):385–8.
[8] De Volder MFL, Tawfick SH, Baughman RH, Hart AJ. Carbon nanotubes: Present and future commercial applications. Science 2013;339:535–9.
[9] Lehtimäki S, Tuukkanen S, Pörhönen J, Moilanen P, Virtanen J, Honkanen M, et al. Low-cost, solution processable carbon nanotube nanocomposite supercapacitors and their characterization 2014;(submitted).
[10] Lehtimäki S, Li M, Salomaa J, Pörhönen J, Kalanti A, Tuukkanen S, et al. Performance of printable supercapacitors in an rf energy harvesting circuit. International Journal of Electrical Power and Energy Systems 2014;(in press).
[11] Kötz R, Carlen M. Principles and applications of electrochemical capacitors. Electrochim Acta 2000;45(15):2483–98.
[12] Li X, Wei B. Supercapacitors based on nanostructured carbon. Nano Energy 2013;2(2):159–73.
[13] Liu Q, Liu Z, Zhang X, Yang L, Zhang N, Pan G, et al. Polymer photovoltaic cells based on solution-processable graphene and P3HT. Adv Funct Mater 2009;19:894–904.
[14] Fan B, Mei X, Sun K, Ouyang J. Conducting polymer carbon nanotube composite as counter electrode of dye-sensitized solar cells. Applied Physics Letters 2008;93:143103.
[15] Wang X, Zhi L, Müllen K. Transparent, conductive graphene electrodes for dye-sensitized solar cells. Nano Letters 2008;8(1):323–7.
[16] Bansal M, Srivastava R, Lal C, Kamalasanan MN, Tanwar LS. Carbon nanotube-based organic light emitting diodes. Nanoscale 2009;1:317–30.
[17] Cao Q, Zhu ZT, Lemaitre MG, Xia MG, Shim M, Rogers JA. Transparent flexible organic thin-film transistors that use printed single-walled carbon nanotube electrodes. Appl Phys Lett 2006;88(11):113511–13.
[18] Tuukkanen S, Julin T, Rantanen V, Zakrzewski M, Moilanen P, Lupo D. Low-temperature solution processable electrodes for piezoelectric sensors applications. Japanese Journal of Applied Physics 2013;52:05DA06.
[19] Kim K, Shin K, Han JH, Lee KR, Kim WH, Park KB, et al. Deformable single wall carbon nanotube electrode for transparent tactile touch screen. Electronics Letters 2011;47(2):118–20.
[20] Wang HH. Chapter 9 - flexible chemical sensors. In: Sun Y, Rogers JA, editors. Semiconductor Nanomaterials for Flexible Technologies. Oxford: William Andrew Publishing; 2010, p. 247–73.
[21] Xiao J, Jiang H, Huang Y, Rogers JA. Chapter 10 - mechanics of stiff thin films of controlled wavy geometry on compliant substrates for stretchable electronics. In: Sun Y, Rogers JA, editors. Semiconductor Nanomaterials for Flexible Technologies. Oxford: William Andrew Publishing; 2010, p. 275–91.
[22] Sekitani T, Someya T. Stretchable, large-area organic electronics. Advanced Materials 2010;22(20):2228–46.
[23] Bokobza L. Multiwall carbon nanotube elastomeric composites: A review. Polymer 2007;48(17):4907–20.
[24] Arias AC, MacKenzie JD, McCulloch I, Rivnay J, Salleo A, et al. Materials and applications for large area electronics: solution-based approaches. Chemical reviews 2010;110(1):3–24.
[25] Forrest SR. The path to ubiquitous and low-cost organic electronic appliances on plastic. Nature 2004;428(6986):911–8.
[26] Hecker K, Breitung S. OE-A Roadmap for Organic and Printed Electronics: White Paper, 4th ed., Organic Electronics Association (OE-A). VDMA Verlag GmbH; 2011,.
[27] Towards a green electronics in europe, the strategic research agenda

(SRA) for the organic and large area electronics (OLAE). Published on the OPERA website on September 18; 2009,.
[28] Wassei JK, Tung VC, Jonas SJ, Cha K, Dunn BS, Yang Y, et al. Stenciling graphene, carbon nanotubes, and fullerenes using elastomeric lift-off membranes. Advanced Materials 2010;22(8):897–901.
[29] Tung VC, Chen LM, Allen MJ, Wassei JK, Nelson K, Kaner RB, et al. Low-temperature solution processing of graphene-carbon nanotube hybrid materials for high-performance transparent conductors. Nano Letters 2009;9(5):1949–55.
[30] Minami N, Kim Y, Miyashita K, Kazaoui S, Nalini B. Cellulose derivatives as excellent dispersants for single-wall carbon nanotubes as demonstrated by absorption and photoluminescence spectroscopy. Applied Physics Letters 2006;88:093123.
[31] Tuukkanen S, Julin T, Rantanen V, Zakrzewski M, Moilanen P, Lilja KE, et al. Solution-processible electrode materials for a heat-sensitive piezoelectric thin-film sensor. Synthetic Metals 2012;162:1987–95.
[32] Murphy R, Coleman JN, Cadek M, McCarthy B, Bent M, Drury A, et al. High-yield, nondestructive purification and quantification method for multiwalled carbon nanotubes. The Journal of Physical Chemistry B 2002;106(12):3087–91.
[33] Hu L, Hecht DS, Grüner G. Carbon nanotube thin films: fabrication, properties, and applications. Chemical reviews 2010;110(10):5790–844.
[34] Yun S, Jang SD, Yun GY, Kim JH, Kim J. Paper transistor made with covalently bonded multiwalled carbon nanotube and cellulose. Applied Physics Letters 2009;95(10):104102.
[35] LeMieux MC, Roberts M, Barman S, Jin YW, Kim JM, Bao Z. Self-sorted, aligned nanotube networks for thin-film transistors. Science 2008;321(5885):101–4.
[36] Bhattacharyya S, Sinturel C, Bahloul O, Saboungi ML, Thomas S, Salvetat JP. Improving reinforcement of natural rubber by networking of activated carbon nanotubes. Carbon 2008;46(7):1037 –45.
[37] Das A, Stöckelhuber K, Jurk R, Fritzsche J, Klüppel M, Heinrich G. Coupling activity of ionic liquids between diene elastomers and multi-walled carbon nanotubes. Carbon 2009;47(14):3313–21.
[38] Likozar B, Major Z. Morphology, mechanical, cross-linking, thermal, and tribological properties of nitrile and hydrogenated nitrile rubbermultiwalled carbon nanotubes composites prepared by melt compounding: The effect of acrylonitrile content and hydrogenation. Applied Surface Science 2010;257(2):565–73.
[39] Peng Z, Feng C, Luo Y, Li Y, Kong L. Self-assembled natural rubber/multi-walled carbon nanotube composites using latex compounding techniques. Carbon 2010;48(15):4497–503.
[40] Ata S, Kobashi K, Yumura M, Hata K. Mechanically durable and highly conductive elastomeric composites from long single-walled carbon nanotubes mimicking the chain structure of polymers. Nano Letters 2012;12(6):2710–6.
[41] Sekitani T, Noguchi Y, Hata K, Fukushima T, Aida T, Someya T. A rubberlike stretchable active matrix using elastic conductors. Science 2008;321(5895):1468–72.
[42] Liu CH, Huang H, Wu Y, Fan SS. Thermal conductivity improvement of silicone elastomer with carbon nanotube loading. Applied Physics Letters 2004;84(21):4248–50.
[43] Hernández M, Bernal MdM, Verdejo R, Ezquerra TA, López-Manchado MA. Overall performance of natural rubber/graphene nanocomposites. Composites Science and Technology 2012;73:40–6.
[44] Bae S, Kim H, Lee Y, Xu X, Park JS, Zheng Y, et al. Roll-to-roll production of 30-inch graphene films for transparent electrodes. Nature nanotechnology 2010;5(8):574–8.
[45] Kim KS, Zhao Y, Jang H, Lee SY, Kim JM, Kim KS, et al. Large-scale pattern growth of graphene films for stretchable transparent electrodes. Nature 2009;457(7230):706–10.
[46] Khang DY, Xiao J, Kocabas C, MacLaren S, Banks T, Jiang H, et al. Molecular scale buckling mechanics in individual aligned single-wall carbon nanotubes on elastomeric substrates. Nano letters 2008;8(1):124–30.
[47] Rogers JA, Someya T, Huang Y. Materials and mechanics for stretchable electronics. Science 2010;327(5973):1603–7.
[48] Mullins L. Softening of rubber by deformation. Rubber Chemistry and Technology 1969;42(1):339–362.
[49] Diani J, Bruno F, Gilormini P. A review on the mullins effect. European Polymer Journal 2009;45:601–612.
[50] Smits F. Measurement of sheet resistivities with the four-point probe. Bell Syst Tech J 1958;37(3):711–8.
[51] Standard Test Methods for Measuring Adhesion by Tape Test. United States ASTM D3359-97. 1997.
[52] Lim SC, Jang JH, Bae DJ, Han GH, Lee S, Yeo IS, et al. Contact resistance between metal and carbon nanotube interconnects: effect of work function and wettability. Applied Physics Letters 2009;95(26):264103.

Table 2: Sheet resistance and adhesion classification before and after stretching experiments. *X* refers to graphene and *Y* to CNT electrodes. The numbers *1–4* refer to the different rubber substrates.

Sample	R_S ($\Omega/\square$)	Adhesion classification before stretching	Adhesion classification after stretching
X-1	180 ± 30	0B	0B
X-2	100 ± 20	3B	2B
X-3	70 ± 10	4B	4B
X-4	70 ± 10	4B	4B
Y-1	120 ± 20	3B	1B
Y-2	140 ± 20	1B	1B
Y-3	110 ± 10	3B	2B
Y-4	90 ± 10	5B	4B

Table 3: Summary of the stretching experiments. Electrode resistance was measured before (R_{before}) and after (R_{after}) the stretching experiment. $R_{\text{final}}/R_{\text{initial}}$ describes the ratio of resistance in the end and in the beginning of the stretching experiment. Calculated gauge factors (GF) and rubber relaxation analysis.

Sample	R_{before} (kΩ)	R_{after} (kΩ)	$R_{\text{final}}/R_{\text{initial}}$	GF	Rubber relaxation
X-2	2.17	8.10	3.8	14	No
X-3	0.16	0.24	1.9	4.5	Yes
Y-1	0.36	0.36	19	90	Yes
Y-2	0.19	0.38	7.7	33	No
Y-3	0.18	0.14	120	590	Yes
Y-4	0.20	0.18	46	220	No

Table 1: Properties of the rubber substrates.

Rubber substrate	Tensile strength (MPa)	Elongation at break (%)	Stress at 100% (MPa)	Shore A hardness (15s)	Surface energy (mN/m)
1	12.9	581	0.86	36.5	11.3 ± 0.2
2	22.8	593	1.3	46	13.7 ± 2.7
3	2.2	540	0.82	35	19.4 ± 2.0
4	7.5	370	2.0	47	23.5 ± 0.2

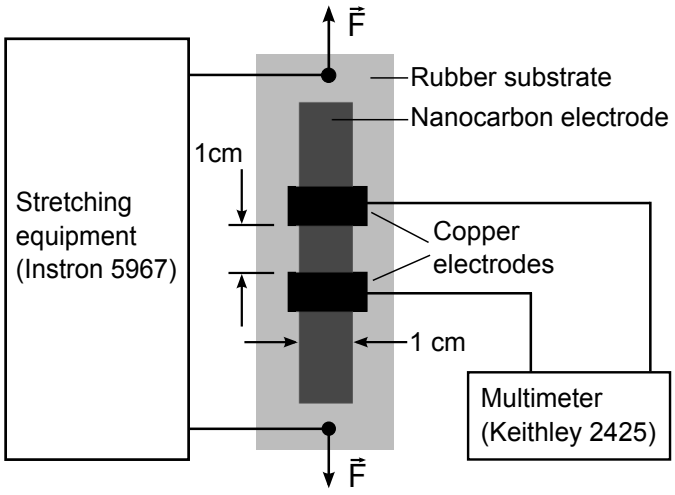

Figure 1: A schematic view of the stepwise stretching measurement setup.

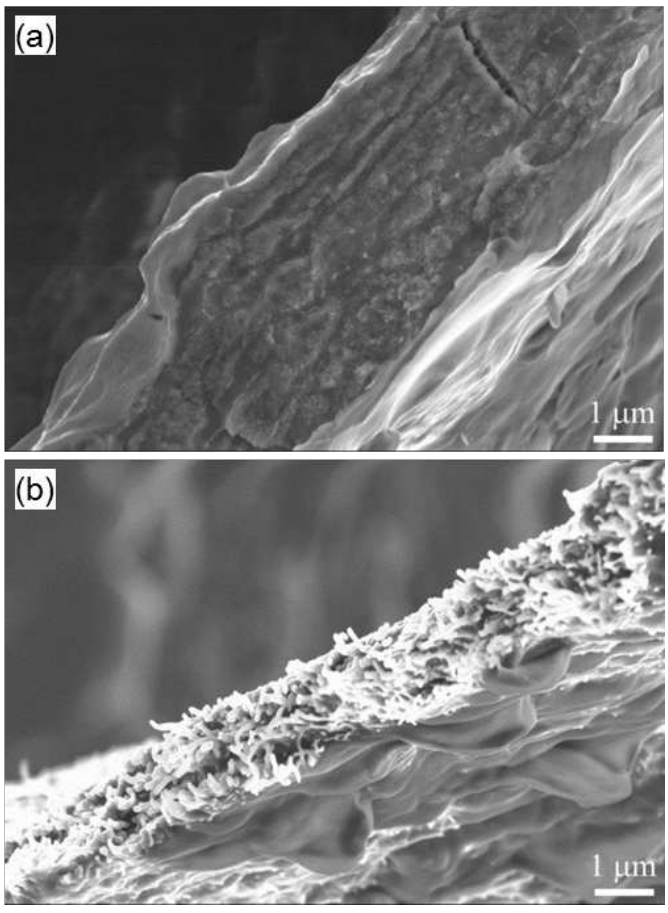

Figure 4: SEM images of the cross-section of the (a) graphene (sample *X-2*) and (b) CNT electrodes (sample *Y-1*) on rubber substrates.

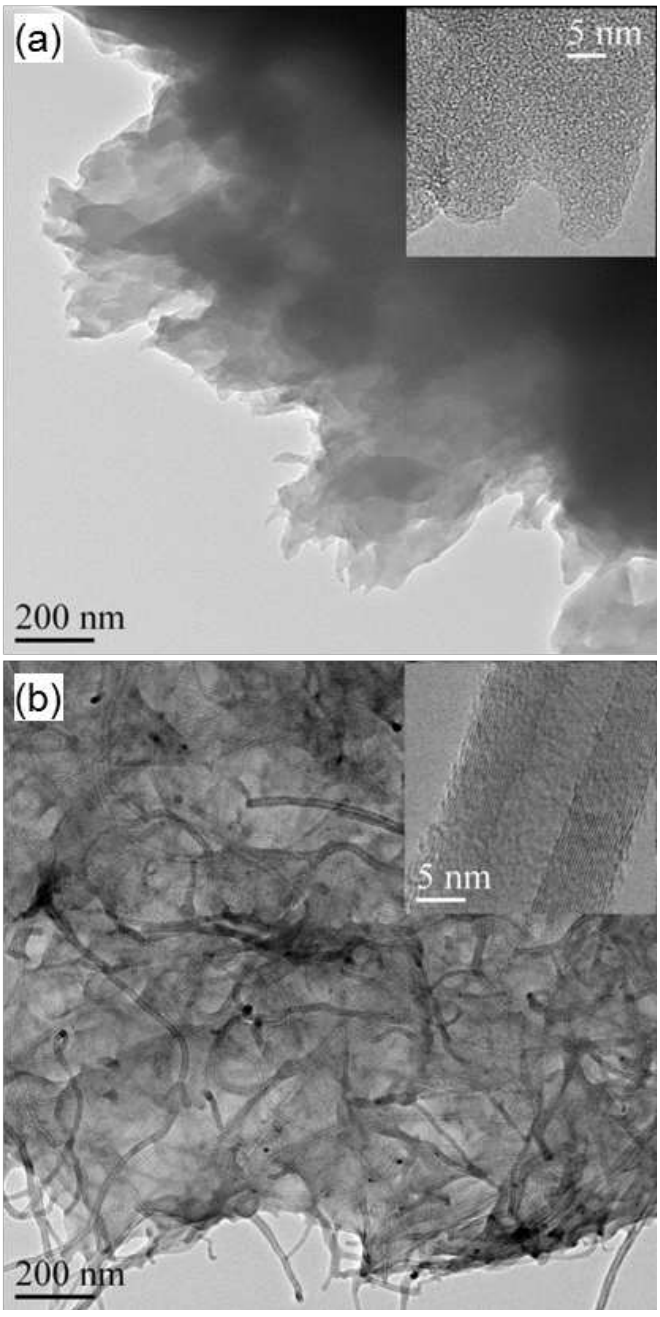

Figure 5: TEM images of (a) graphene (sample *X-3*) and (b) CNT (sample *Y-1*) electrode materials.

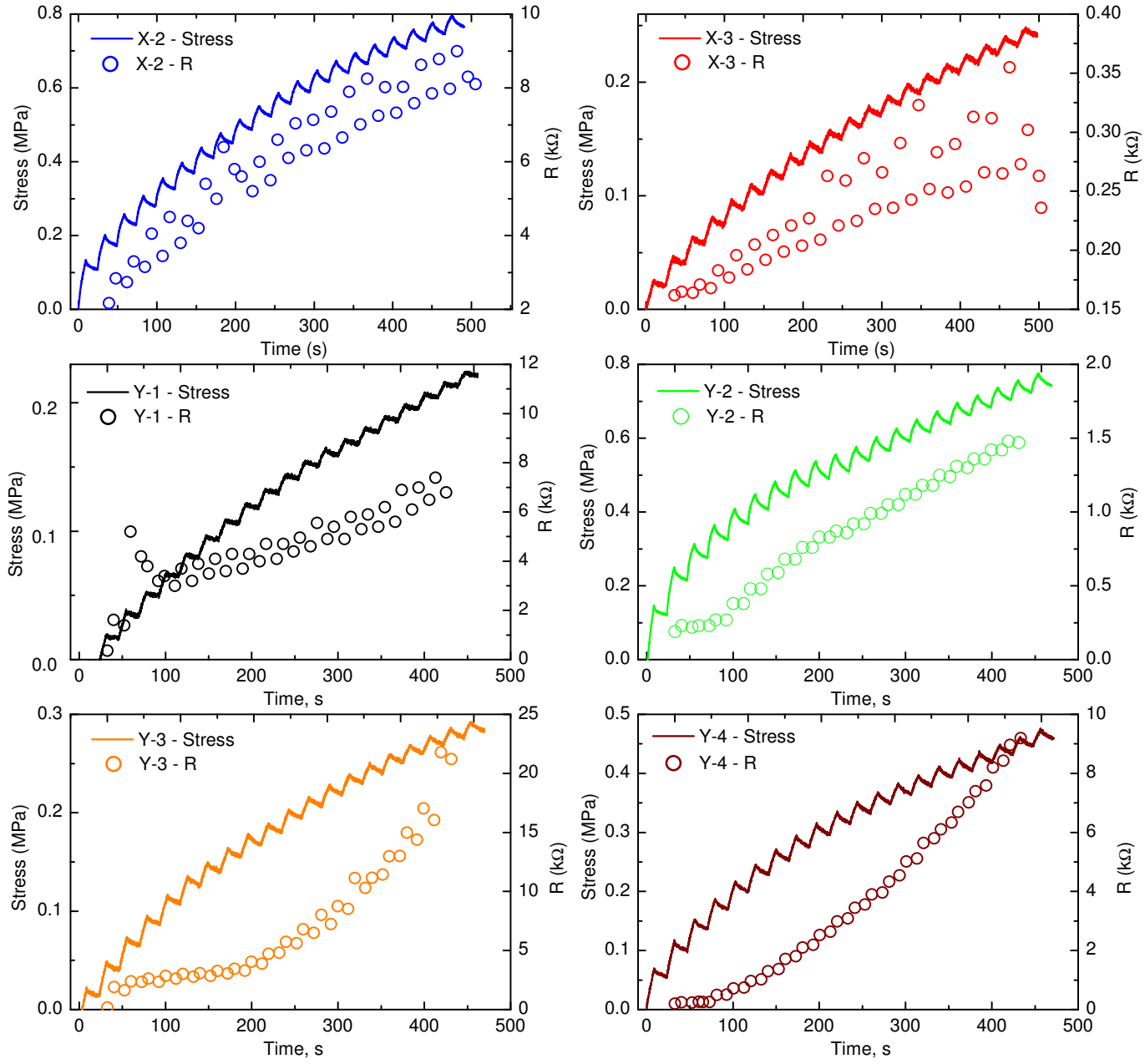

Figure 2: Measured stress and resistance as a function of time during the stepwise stretching experiments. The resistances where collected in the beginning and in the end of each pause between stretching steps. Zig-zag shape in the stress curves is due to the rubber relaxation between the stretching steps.

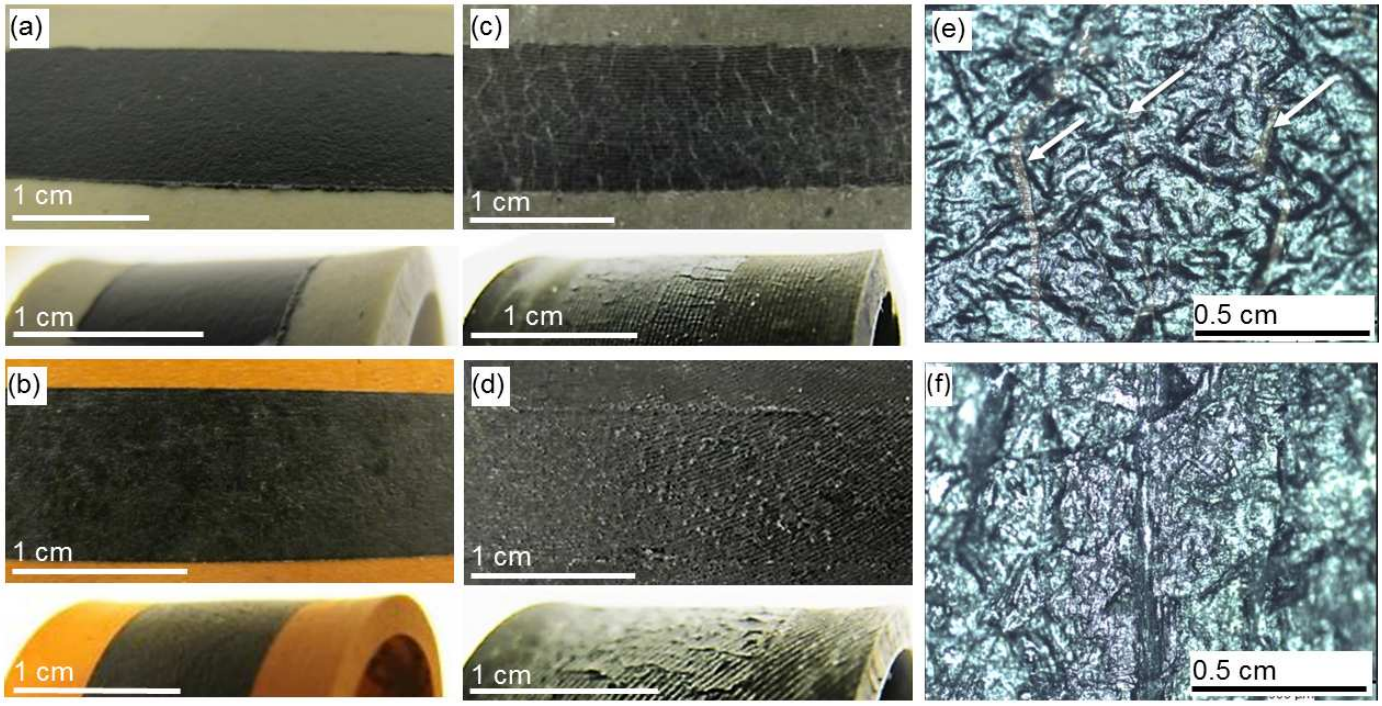

Figure 3: Photographs of the samples (a) *X-3*, (b) *Y-4*, (c) *X-1* and (d) *X-2*. The upper and lower present the sample as straight and as bent, respectively. Micrographs of samples (e) *X-4* and (f) *Y-1* after the stretching experiments. Arrows in (e) are pointing at the deep cracks.